

# The Effect of Temperature and Deformation Rate on the Hot-Drawing Behavior of Porous High-Molecular-Weight Polyethylene Fibers

J. SMOOK and A. J. PENNINGGS, *Department of Polymer Chemistry, State University of Groningen, Nijenborgh 16, Groningen, The Netherlands*

## Synopsis

The nature of the deformation process involved in hot drawing of porous high-molecular-weight polyethylene was examined by apparent elongational viscosity measurements at drawing temperatures between 100°C and 150°C and deformation rates in the range of  $10^{-6}$ – $10^{-3}$  m/s. The temperature dependence of the apparent elongational viscosity revealed three distinguishable intervals with different activation energies. In the range of 100–133°C, the activation energy amounted to 50 kJ/mol, indicating that hot-drawing in this region proceeds by a sliding motion of separate fibrillar units. The interval between 133°C and 143°C was characterized by an activation energy of about 150 kJ/mol. Moreover, the porous character of the polyethylene fibers was found to decrease in the drawing process above 133°C. These observations were ascribed to an aggregation of the elementary fibrils upon hot-drawing due to partial melting at the surface of the fibrils. At temperatures above 143°C the activation energy was strongly affected by the initial morphology and the draw ratio of the fibers and amounted to values in the range of 200–600 kJ/mol. Molecular orientation in this region is accomplished by a slippage of individual chains, with entanglements acting as semipermanent crosslinks. Decreasing of the rate of elongation in the drawing process resulted in premature fiber breakage, indicating that the crosslinking action of the entanglements is limited by the time scale of the process.

## INTRODUCTION

The extensive activity during the last decade in the field of ultraoriented polymeric structures has resulted in a rapid development of new strong materials, such as carbon fibers,<sup>1</sup> poly(*p*-phenyleneterephthalamide) fibers (Kevlar 49,<sup>2</sup> Arenka<sup>3</sup>) and ultrahigh strength polyethylene fibers.<sup>4–6</sup> In recent papers<sup>6–8</sup> from our laboratory we have shown that porous high-molecular-weight polyethylene can be employed successfully to generate high strength fibers with a tensile strength at break up to 4.1 GPa and a Young's modulus up to 120 GPa.

The porous fibers were obtained by spinning a semidilute solution of the polyethylene in paraffin–oil followed by extraction of the solvent. In a subsequent step the porous fibers were hot-drawn at a drawing temperature of 148°C. The greatly enhanced drawability of the porous fibers, as compared to melt-processed high-molecular-weight polyethylene,<sup>9</sup> was discussed in terms of a favorable molecular topology. Fiber preparation, started from semidilute solutions of the high-molecular-weight polyethylene, results in a considerable reduction of the number of defects, such as trapped entanglements, interwinings, chain ends, kinks, jogs, etc. These topological defects impede the alignment of the molecules during drawing and reduce the ultimate tensile strength of the fibers.<sup>10</sup> After extraction, a loosely connected lamellar network is formed, showing a high porosity. Additionally, the large free volume and the high surface-free energy in this structure are also factors that promote a high drawability.

The mechanism by which the alignment of the molecules is accomplished in the drawing process is, however, still rather obscure. A better understanding of the deformation process can be provided by examining the activation process involved in drawing.<sup>11,12</sup> A quantity that is strongly affected by the deformation mechanism is the elongational viscosity  $\eta_e$ , which can be considered characteristic for a material and correlatable to molecular structure, molecular weight, molecular weight distribution, and spinnability of a material.<sup>13</sup> From the temperature dependence of  $\eta_e$  the activation energy of the drawing process can be estimated, and additional information about the molecular orientation may be obtained from the dependence of elongational viscosity on deformation rate  $\dot{\epsilon}$  and draw ratio  $\lambda$ .

The main objective of this investigation was the experimental determination of elongational viscosity  $\eta_e$  during hot-drawing of porous high-molecular-weight polyethylene fibers as a function of deformation rate and draw ratio in the temperature range of 100–150°C. Three different temperature regions were observed with a different value for the activation energy of the drawing process. Drawing experiments were carried out with slow tensile speeds in the range of  $10^{-6}$ – $10^{-3}$  m/s. It was noticed that a decrease of the tensile speed resulted in decreasing draw ratio due to fiber fracture. The experimental results indicated that drawing of the porous polyethylene fibers at temperatures below 143°C proceeds by a sliding motion of separate fibrils. As the temperature exceeds 143°C, individual chains are slipping past each other in the drawing process, with entanglements acting as semipermanent crosslinks.

### THEORETICAL ASPECTS

The rheological equation of state describes the dependence between the state of stress in a system and the components of deformation<sup>13</sup>:

$$\tau = f(\mathbf{D}) \quad (1)$$

where  $\tau$  is the stress tensor and  $f(\mathbf{D})$  denotes some function of the rate of deformation tensor  $\mathbf{D}$ . In the past much effort has been put into deriving theoretical expressions for the elongational viscosity in polymeric systems from different forms of constitutive equations.<sup>14–18</sup> For a Newtonian fluid the constitutive equation simply reads

$$\tau = \eta \mathbf{D} \quad (2)$$

where  $\eta$  is the viscosity. In the case of a steady uniaxial extensional flow field (directed along the  $x$ -axis) for an incompressible fluid the rate of deformation tensor is given by

$$\mathbf{D} = \begin{pmatrix} \dot{\epsilon} & 0 & 0 \\ 0 & -1/2\dot{\epsilon} & 0 \\ 0 & 0 & -1/2\dot{\epsilon} \end{pmatrix}, \quad \text{with } \dot{\epsilon} = \frac{dv_x}{dx} \quad (3)$$

As a result, the elongational viscosity  $\eta_e$  is determined by the scalar equation

$$\eta_e = \frac{\sigma_{xx}}{\dot{\epsilon}} \quad (4)$$

where  $\sigma_{xx} = F_{xx}/A_{xx}$  = axial tensile stress,  $F_{xx}$  = axial tensile force,  $A_{xx}$  = cross section at place  $x$ ,  $\dot{\epsilon} = dv_x/dx = (1/\lambda) \cdot (d\lambda/dt)$  = deformation rate,  $\lambda$  = draw ratio. For the elongational viscosity a thermally activated process can be expected according to the Eyring-Frenkel equation<sup>19</sup>:

$$\eta_e(T) = \eta_e(T_0) \cdot \exp \left[ \frac{E_a}{R} \left( \frac{1}{T} - \frac{1}{T_0} \right) \right] \quad (5)$$

where  $E_a$  is an activation energy and  $R$  is the gas constant.

### Elongational Viscosity in Relation to Deformation Rate

For Newtonian liquids the elongational viscosity  $\eta_e$  is three times the shear viscosity  $\eta_0$  as was first revealed by Trouton.<sup>20</sup> In polymeric substances, however, the situation is more complex as the viscosity is strongly dependent on the deformation rate and the relation  $\eta_e = 3\eta_0$  is only a limiting condition at low stretching rates. Ever since elongational viscosity has been determined in polymers, much confusion has existed about the relation between  $\eta_e$  and deformation rate  $\dot{\epsilon}$ , mainly due to the very complicated nature of elongational flow behavior of fiber-forming polymers.

Experimental determination of elongational viscosity under constant deformation rate conditions in polymeric materials generally reveals an increasing value of  $\eta_e$  with elongation rate<sup>13</sup> in accordance with theoretical predictions.<sup>14-18</sup> However, White<sup>21,22</sup> reported steady-state elongational viscosity data on high-density polyethylene and polypropylene showing a decreasing value of  $\eta_e$  with deformation rate. Many efforts have been made to analyze the elongational flow behavior of polymeric materials in the melt spinning process.<sup>19,23-25</sup> However, in melt spinning the elongational rate varies along the spinway. As a result the experimentally determined elongational viscosity does not conform to the definition of "steady" elongational viscosity<sup>13</sup> and is sometimes denoted as "apparent" elongational viscosity. For melt spinning of polymers it was observed that  $\eta_e$  can increase, decrease, or remain constant with deformation rate  $\dot{\epsilon}$ , depending on the material being spun and the behavior of deformation rate along the spinway.<sup>13,21</sup> In order to overcome the discrepancy between observed experimental results for the elongational viscosity with deformation rate  $\dot{\epsilon}$  and theoretical predictions,<sup>14-18</sup> based on the assumption of constant elongation rate conditions, Lamonte and Han<sup>26</sup> introduced an empirical equation for the elongational viscosity in relation to deformation rate

$$\eta_e = 3\eta_0 \left[ a + b \left( \frac{dv_x}{dx} \right)^{q-1} \right] \quad (6)$$

where  $a$ ,  $b$ , and  $q$  are constants characteristic of the material. Depending on the values of  $a$ ,  $b$ , and  $q$ , elongational viscosity can increase, decrease, or remain constant with deformation rate. Recently Doi and Edwards<sup>27-30</sup> derived mathematical expressions for the rheological properties of the polymer melt, based on the concept of "reptation" as introduced by de Gennes.<sup>31</sup> Marrucci and Hermans<sup>32</sup> modified the Doi-Edwards theory and obtained an expression for  $\eta_e$ , which showed a maximum as a function of  $\dot{\epsilon}$ . This last model is thus capable of explaining observed experimental results for elongational viscosity vs. deformation rate in polymer melts. During the process of hot drawing, however,

a more complex behavior is to be expected since the material exists in a semi-crystalline state. The above-mentioned models are, strictly speaking, only applicable to the melt. Nevertheless, some aspects of these models may be used to discuss the observed experimental results on hot-drawing of porous high-molecular-weight polyethylene in terms of flow units, which are composed of several molecules.

### Elongational Viscosity in Relation to Temperature

Measurements of elongational viscosity  $\eta_e$  during the melt spinning process of polymers<sup>23,24</sup> have been criticized<sup>33</sup> as it is not possible to separate the effect of rate of elongation and temperature due to nonisothermal effects. Accordingly, it becomes clear that, in order to determine  $\eta_e$  as a function of temperature, isothermal conditions have to be maintained.<sup>25,26</sup> A complicating factor in this respect is that during drawing the work of deformation is almost completely converted into heat,<sup>34</sup> which may cause self-heating of the sample. Nevertheless, if the elongation occurs at a low enough deformation rate, the heat produced can be dissipated entirely to the surrounding atmosphere of the sample.<sup>35</sup> Further complications may be brought about by the occurrence of a "memory effect" in polymers.<sup>36</sup> Former processing conditions will affect the deformation behavior of polymeric samples. Therefore, processing conditions have to be standardized in order to establish the dependence of elongational viscosity on temperature.

The temperature dependence of elongational viscosity results in a value for the activation energy of the deformation process, from which it may be possible to obtain information about several molecular processes. Recently Mead and Porter<sup>37</sup> reported data on the determination of an "apparent" elongational viscosity during the solid-state extrusion of polyethylene. The activation energy, as determined from  $\eta_e$  vs.  $T^{-1}$ , enabled them to correlate the observed behavior of polyethylene in solid-state extrusion with the so-called  $\alpha_c$  relaxation in polyethylene.<sup>38,39</sup> Therefore, it is our belief that determination of the activation energy for the hot drawing of porous high-molecular-weight polyethylene might give a further insight into the deformation mechanism of this process.

Several authors have been dealing with this subject from a more theoretical point of view. Peterlin<sup>12</sup> proposed a mechanism in which lamellae are transformed into microfibrils, followed by a longitudinal sliding motion of microfibrils past each other. The longitudinal sliding of the microfibrils proceeds by a translational displacement of a whole straight section of the molecules, comprising about 80 monomer units in polyethylene. This assumption leads to an activation energy between 200 and 300 kJ/mol. Clark and Scott<sup>40</sup> introduced the concept of "superdrawing," involving migration of crystal defects through the crystal lattice. Reneker<sup>41</sup> suggested point dislocations to move along the chain in the crystal lattice, resulting in an axial displacement of the molecules as a whole. The Reneker process proceeds with a considerably lower activation energy than the one calculated by Peterlin.<sup>12</sup> Furthermore, it has been recognized that the onset of the  $\alpha_c$ -relaxation<sup>38,39</sup> can be correlated with the motions of the molecules during orientation.

TABLE I  
Sample Details

| Sample | Polymer | Spinning solution (wt %) | Extrusion temp (°C) | Extrusion rate (m/min) | Cross section (m <sup>2</sup> ) |
|--------|---------|--------------------------|---------------------|------------------------|---------------------------------|
| A      | Hi-fax  | 5% in paraffin-oil       | 170                 | 1.0                    | $2.4 \times 10^{-8}$            |
| B      | Hi-fax  | 5% in paraffin-oil       | 170                 | 0.6                    | $3.3 \times 10^{-8}$            |
| C      | Hi-fax  | 3% in paraffin-oil       | 170                 | 1.5                    | $1.1 \times 10^{-8}$            |

## EXPERIMENTAL

### Samples

High-molecular-weight polyethylene Hi-fax 1900, with  $\bar{M}_w = 4 \times 10^6$  and  $\bar{M}_n = 2 \times 10^5$  was used. The preparation of the porous as-spun polyethylene fibers has been described in detail previously.<sup>7,8</sup> For the present study a series of three different porous fiber materials was produced the characteristics of which are shown in Table I.

### Dynamometer

The drawing experiments for the determination of elongational viscosity were carried out in a dynamometer,<sup>42</sup> in which short samples with an initial length of 2.5 cm were elongated at a constant tensile speed. The load cell (Statham Instruments, Model UC3 equipped with a UL5 load cell accessory) has a measuring range of 0–220 g. Ten fixed tensile speeds were available, ranging from  $10^{-3}$  m/s up to  $10^{-6}$  m/s. Since the tensile speeds were fixed, the experiments could not be performed at a constant rate of deformation, as is actually desired for the determination of elongational viscosity. However, the rate of deformation also changes during standard hot-drawing procedures<sup>8</sup> of fibers in praxis. Nevertheless it should be realized that the elongational viscosity, as determined throughout this study, does not correspond with the definition of “steady” elongational flow<sup>13</sup> and will further on be referred to as “apparent” elongational viscosity  $\eta_e$ . The temperature throughout the glass vessel of the dynamometer was constant within 0.5°C. Temperature was measured in the direct vicinity of the sample by means of a resistor thermometer (Pt 100). In order to prevent oxidative degradation, nitrogen was allowed to flow through the glass vessel at a moderate rate.

### Experimental Determination of “Apparent” Elongational Viscosity

In the course of the experimental study plots were obtained of the axial tensile force  $F_{xx}$  vs. time during the elongation of the porous polyethylene fibers. The cross section of the fiber at each moment was calculated from the original cross section  $A_0$  and the draw ratio  $\lambda(t)$  at time  $t$ , according to

$$A(t) = A_0/\lambda(t) \quad (7)$$

and

$$\lambda(t) = (L_0 + vt)/L_0 \quad (8)$$

where  $L_0$  is the original sample length and  $v$  is the tensile speed. As a result, the axial tensile stress  $\sigma(t)$  is given by

$$\sigma(t) = F_{xx}/A(t) \quad (9)$$

The deformation rate at each moment  $\dot{\epsilon}(t)$  was determined as follows,

$$\dot{\epsilon}(t) = \frac{1}{L} \cdot \frac{dL}{dt} = \frac{v}{L_0 + vt} \quad (10)$$

With these variables the "apparent" elongational viscosity  $\eta_\epsilon = \sigma(t)/\dot{\epsilon}(t)$  could be calculated for each value of the draw ratio  $\lambda$ .

### Experimental Precautions

The best results in clamping the porous high-molecular-weight polyethylene fibers were obtained with modified battery clamps (Fig. 1), which were sand-blasted in order to prevent slippage. Cross-sectional areas of the porous as-spun fibers were determined from fiber weight and length assuming a density of 1000 kg/m<sup>3</sup>. All the porous fibers were slightly predrawn (materials A and B: initial draw ratio 5.3; material C: initial draw ratio 4.6) before elongational viscosity measurements were started in the dynamometer. If porous as-spun fibers were drawn at temperatures below ca. 130°C, it was noticed that nonhomogeneous deformation took place at small draw ratios. Drawing of as-spun fibers above 130°C was impossible because the fibers were melted before elongation was started, as a consequence of their lamellar nature. The predrawing of the porous fibers occurred in the standard drawing apparatus, described previously,<sup>8</sup> in which a temperature gradient was applied to avoid neck formation in the drawing process. The highest temperature of the gradient was taken equal to the drawing temperature in the dynamometer. To get isothermal conditions established, it was necessary to wait some time after clamping of the samples before the elongation was initiated. A period of 15 min was found to be sufficient in order to obtain good reproducibility.

### Effect of Deformation Work

The tensile speeds during the drawing of the porous polyethylene fibers were chosen to be in the range of 10<sup>-6</sup>-10<sup>-3</sup> m/s, so as to avoid self-heating of the samples due to internal friction.<sup>34</sup> However, the measured values for the "ap-

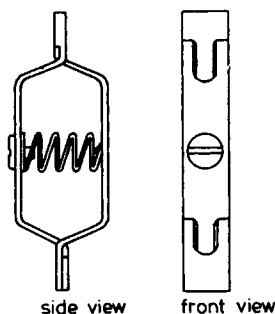


Fig. 1. Schematic representation of modified battery clamps.

parent" elongational viscosity were found to be extremely high, namely in the range of  $10^9$ – $10^{12}$  Poises. In view of these high values it was considered necessary to estimate the heating effects in the drawing process, to establish whether the assumption of isothermal conditions was justified. In the literature it was shown<sup>43</sup> that so-called "adiabatic" drawing could be accompanied by a temperature increase up to 20°C of the polymer.

The energy balance for an isotropic material with density  $\rho$ , specific heat  $C_v$ , and thermal conductivity  $\Lambda$  is given by<sup>35</sup>

$$\frac{D}{Dt} (\rho C_v T + U) = \nabla(\Lambda \Delta T) + \text{tr}(\tau \nabla V) \quad (11)$$

where  $\tau$  is the stress tensor,  $U$  the internal energy,  $V$  the velocity, and  $D/Dt$  represents the operator for material time differentiation. A rigorous solution of the equation given above is not available. As a consequence, a more simplified model needs to be considered to assess the heating effects of the drawing process. In the simplified model the fiber is assumed to be a cylindrical sample of length  $l$  and diameter  $d$  in contact with an ambient temperature  $T_\infty$ . The temperature  $T$  throughout the sample is assumed to be uniform. Elongation of the sample is initiated by applying a tensile force which results in a deformation rate  $\dot{\epsilon}$  and a tensile stress  $\sigma$ . Heat transfer through the side surface of the sample is assumed to proceed by convection, while through the front layers with thickness  $dl$  conduction occurs.

The resulting energy balance is

$$\rho C_p \left( \frac{dT}{dt} \right) = \sigma \dot{\epsilon} - \dot{U} - 4\alpha \frac{(T - T_\infty)}{d} - 2 \frac{\Lambda(T - T_\infty)}{ldl} \quad (12)$$

where  $\sigma \dot{\epsilon}$  is the total energy of deformation,  $\sigma \dot{\epsilon} - \dot{U}$  is the dissipative part of this energy, and  $\alpha$  is a heat transfer coefficient. In the underlying case of hot-drawing porous polyethylene fibers, neck formation was avoided in the deformation process. As a result, heat transfer is controlled by convection through the large side surfaces and conduction through the front layers can be neglected. In viscoelastic systems normally part of the deformation energy is stored (elastic energy<sup>44,45</sup>). For the purpose of estimating the maximum temperature increase of the fibers, we assumed that all of the deformation energy was dissipated and the dissipated energy is given by  $\eta_e \dot{\epsilon}^2$ . During the elongation the diameter of the fibers changes. However, the diameter at each time  $t$  can be calculated according to

$$d(t) = \left[ \frac{4}{\pi} A(t) \right]^{1/2} = \left[ \frac{4A_0}{\pi \lambda(t)} \right]^{1/2} = \left[ \frac{4L_0 A_0}{\pi(L_0 + vt)} \right]^{1/2} \quad (13)$$

Hence the energy balance for the case of hot-drawing porous high-molecular-weight polyethylene fibers becomes

$$\rho C_p \left( \frac{dT}{dt} \right) = \eta_e \cdot \dot{\epsilon} - 4\alpha \left( \frac{4L_0 A_0}{\pi} \right)^{-1/4} (L_0 + vt)^{1/2} (T - T_\infty) \quad (14)$$

Furthermore, the energy of deformation per unit time  $\eta_e \dot{\epsilon}^2$  was taken constant during the stretching of the fibers, which was more or less the case for the dy-

namometer experiments. Typical values for the variables in eq. (14) for polyethylene were taken:

$$\begin{aligned}\rho &= 1000 \text{ kg/m}^3 \\ C_p &= 1900 \text{ J/kg}\cdot\text{K}^{46} \\ \alpha &= 60 \text{ J/m}^2\cdot\text{s}\cdot\text{C}^{35}\end{aligned}$$

The value for the heat transfer coefficient  $\alpha$  is rather arbitrary, as it is probably affected by the porosity and the anisotropic character of the fibers. The differential equation given above could not be solved analytically and was therefore solved numerically for some typical values of  $\eta_\epsilon\text{-}\dot{\epsilon}^2$ ,  $L_0$ ,  $\nu$ , and  $T_\infty$  that were met during the experiments. For all cases the calculated temperature increase of the fibers was less than  $0.2^\circ\text{C}$ , which justifies the assumption of constant temperature within the dynamometer experiments.

### Tensile Testing

Tensile tests were carried out using a Zwick Z1.3B tensile tester at a cross-head speed of  $2 \times 10^{-4}$  m/s and an original sample length of 2.5 cm at  $20^\circ\text{C}$ .

## RESULTS

### Effect of Temperature on Hot Drawing of Porous High-Molecular-Weight Polyethylene

To examine the effect of temperature on the drawing properties of the porous polyethylene fibers, a set of drawing experiments was carried out in the standard

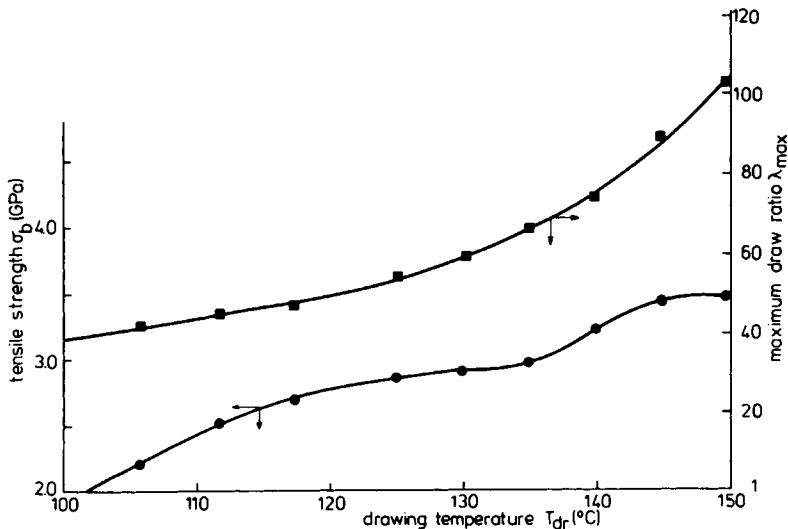


Fig. 2. Tensile strength at break  $\sigma_b$  after drawing to the maximum draw ratio as well as the maximum draw ratio  $\lambda_{max}$  as a function of drawing temperature  $T_{dr}$  for porous high molecular weight polyethylene fibers, corresponding to material A in Table I.



drawing apparatus, as described previously.<sup>8</sup> Figure 2 shows a plot of the tensile strength at break  $\sigma_b$  and the maximum draw ratio  $\lambda_{\max}$  as a function of drawing temperature for fibers of material A. It is seen in Figure 2 that  $\sigma_b$  as well as  $\lambda_{\max}$  gradually increases with drawing temperature up to a maximum value for  $\sigma_b$  of 3.4 GPa at a temperature of 150°C and a draw ratio  $\lambda_{\max}$  of 100. Elongation at temperatures above 150°C gives rise to inferior tensile properties, as was noticed in former experimental studies,<sup>8,47</sup> due to a solid–solid phase transition in oriented high-molecular-weight polyethylene of the orthorhombic phase to a hexagonal one.<sup>47,48</sup>

A significant feature of Figure 2 is the more rapid increase of  $\lambda_{\max}$  above a temperature of ca. 135°C as well as the occurrence of a deflection point in the curve of  $\sigma_b$  vs. temperature around 135°C. Furthermore, it was observed visually that the original white, opaque character of the as-spun porous fibers was preserved in the course of the drawing process below this temperature. When the temperature exceeded 135°C, a more transparent appearance of the polyethylene fibers was developed upon drawing. These observations could be correlated with the porosity of the drawn fibers. In Figure 3 the porosity of fibers, which were drawn to a fixed value of  $\lambda = 40$ , at several temperatures, is presented. At drawing temperatures below 135°C, the original porosity of the as-spun fibers is maintained throughout the drawing process. However, fibers drawn at temperatures exceeding 135°C exhibit a decrease in porosity and more strongly as temperature increases.

Hot drawing is accompanied by a transformation of the original lamellar network into a highly oriented fibrillar structure. The above-mentioned observations may originate from a definite change of the flow patterns in the fibrillar structure during hot drawing, which may involve, e.g., oriented crystallization, mobility of defects under stress, solid state transitions, etc. However, more pronounced information on this subject was supplied by the elongational viscosity measurements in a dynamometer.<sup>42</sup>

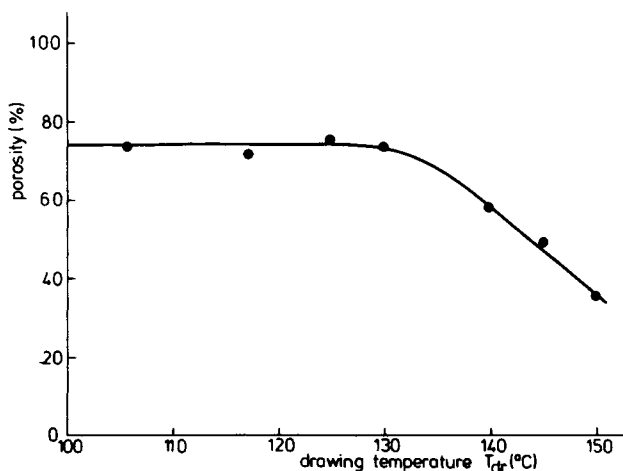


Fig. 3. Porosity of hot-drawn fibers (material A), that were elongated to a fixed draw ratio  $\lambda = 40$  at several temperatures.

### Dependence of "Apparent" Elongational Viscosity on Drawing Temperature

Figure 4 shows the "apparent" elongational viscosity  $\eta_\epsilon$  vs. draw ratio  $\lambda$  for the elongation of fibers of material A at several drawing temperatures. In all cases the fibers were predrawn to  $\lambda = 5.3$  and the tensile speed was  $2 \times 10^{-4}$  m/s. For the sake of clarity it should be noted that the maximum value of the draw ratio  $\lambda_{\max} = 35$  was limited by the length of the dynamometer. At each temperature the apparent elongational viscosity first strongly increases with draw ratio up to  $\lambda = 8$ , whereas at higher values of  $\lambda$  the increase of  $\eta_\epsilon$  is less pronounced. It is interesting to note that the observed behavior of  $\eta_\epsilon$  with  $\lambda$  upon drawing of the porous high-molecular-weight polyethylene fibers is strongly different from the way  $\eta$  develops with  $\lambda$  in the course of solid state extrusion of polyethylene.<sup>37</sup> In that case  $\eta_\epsilon$  increases only slightly at small values of  $\lambda$ . The subsequent "superdrawing"<sup>40</sup> of the solid state extruded polyethylene at higher draw ratios was accompanied by a strong increase of the elongational viscosity. The different behavior in both processes reflects the strong dependence of  $\eta_\epsilon$  on the molecular topology of the fibers. Conversely, molecular topology strongly affects the deformation behavior during the elongation of the polyethylene fibers.

The activation energy for the drawing process  $E_a$  as determined from the dependence of  $\ln \eta_\epsilon$  on  $T^{-1}$  will give information concerning the nature of the deformation. As  $\eta_\epsilon$  is strongly affected by draw ratio as well as deformation rate, it was considered necessary to compare  $\eta_\epsilon$  at a fixed value of  $\lambda$  and  $\dot{\epsilon}$  at each temperature to get a proper estimate of the activation energy. The elongation experiments of the porous polyethylene fibers in the dynamometer were accompanied by a decreasing value of  $\dot{\epsilon}$  with increasing draw ratio; however, each draw ratio corresponded with a fixed  $\dot{\epsilon}$ . In Figure 5  $\ln \eta_\epsilon$  is plotted against  $T^{-1}$

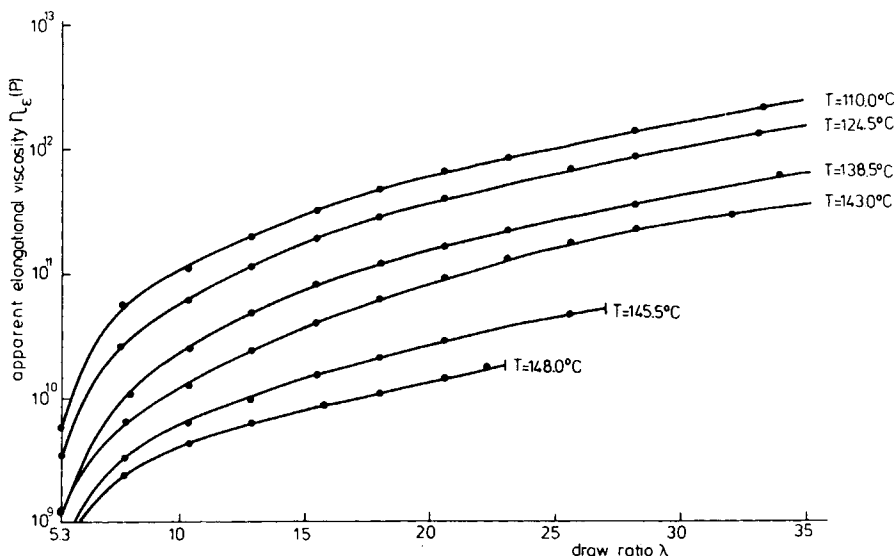


Fig. 4. "Apparent" elongational viscosity  $\eta_\epsilon$  vs. draw ratio  $\lambda$  upon drawing porous polyethylene fibers (material A) at various temperatures (SI units: 1 poise = 0.1 Pa·s).

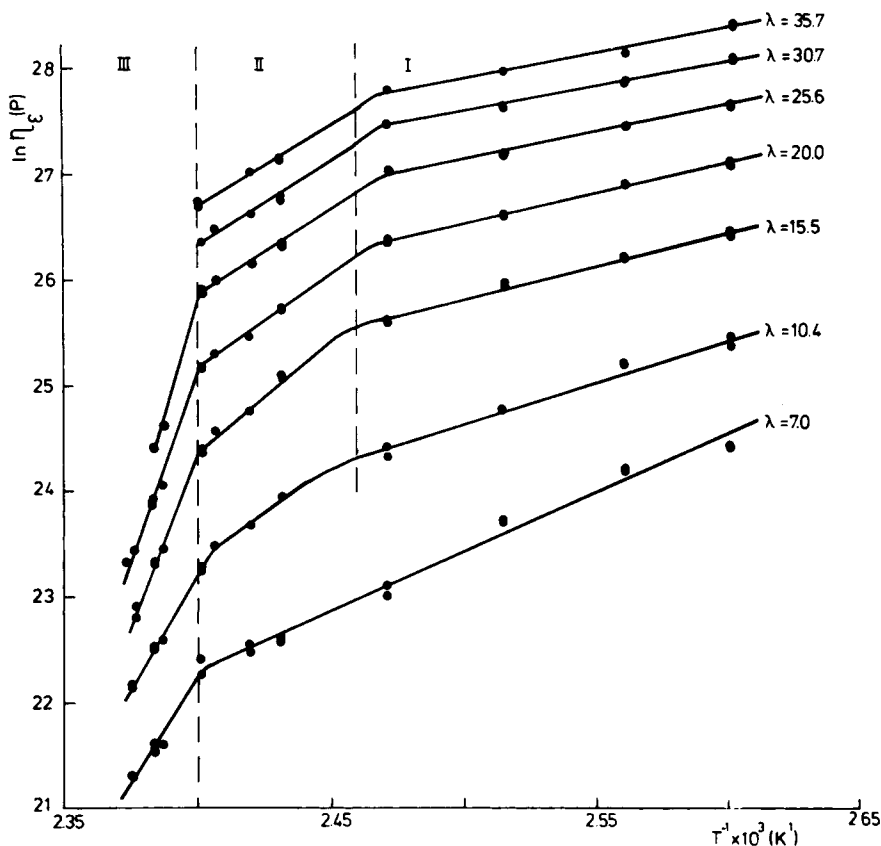


Fig. 5. Plot of logarithm of "apparent" elongational viscosity in  $\eta_e$  vs. reciprocal temperature  $T^{-1}$  at several draw ratios (fiber material A) for the determination of activation energy  $E_a$ .

for porous polyethylene fibers of material A for several draw ratios. Three different temperature regions, characterized by a linear relationship of  $\ln \eta_e$  vs.  $T^{-1}$ , were observed for all values of  $\lambda$ , except the lowest one,  $\lambda = 7$ . A low temperature region up to  $133^\circ\text{C}$  was found, a second region ranged between  $133^\circ\text{C}$  and  $143^\circ\text{C}$ , and finally a high temperature region above  $143^\circ\text{C}$  did occur. All the measurements at different values of  $\lambda$  were duplicated and found to be completely reproducible. At the smallest draw ratio,  $\lambda = 7$ , the distinction between the lowest two temperature regions, however, was not observed for fibers of material A. On the other hand, repeating the experiments with a different set of fibers (material C) did not reveal this deviating behavior at small draw ratios. Apparently the absence of a breaking point in the curves of  $\ln \eta_e$  vs.  $T^{-1}$  at small values of  $\lambda$  is susceptible to small variations in the initial morphology of the fibers.

Figure 6 shows the activation energy  $E_a$ , as calculated from the slope of the straight lines in Figure 5, as a function of draw ratio for both porous fibers of material A and C, which were spun from solutions that were different in the original concentration of the polyethylene. In the lowest temperature region of  $100$ – $133^\circ\text{C}$  the activation energy  $E_a$  decreases slightly with increasing draw ratio in the range of  $35$ – $55$  kJ/mol for both materials. Above  $133^\circ\text{C}$  the nature of the deformation process has changed, as was already suggested in view of the

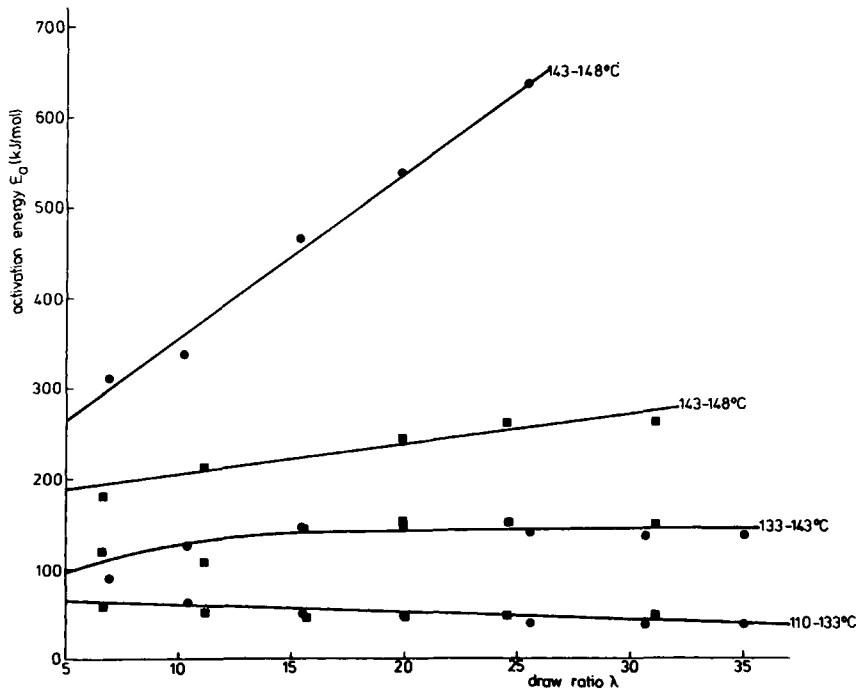


Fig. 6. Activation energy  $E_a$  as a function of draw ratio  $\lambda$  for both porous fibers: (●) Material A spun from 5% solution, (■) material C spun from 3% solution.

porosity changes that take place during hot drawing. In the range between 133°C and 143°C,  $E_a$  slightly increases with  $\lambda$  from 120 kJ/mol up to 150 kJ/mol at  $\lambda = 15$ . At larger draw ratios the activation energy remains constant at 150 kJ/mol.

When the temperature exceeds 143°C up to 148°C, which was the highest temperature at which  $\eta_e$  was determined, the activation process seems to have strongly changed. For both fiber materials A and C, the activation energy was found to be strongly dependent on draw ratio. The porous fibers of material A that were spun from the most concentrated spinning solution (5%) showed values of  $E_a$  increasing with  $\lambda$  in the range of 300–600 kJ/mol. In the case of material C (3% spinning solution) the dependence of  $E_a$  on the draw ratio was somewhat less pronounced and values of  $E_a$  ranged between 180 and 250 kJ/mol. The occurrence of the temperature region for the activation process above 143°C may be brought about by the phase transition of the orthorhombic to the hexagonal phase<sup>48,49</sup> in high-molecular-weight polyethylene, which may have shifted to a somewhat lower temperature due to the drawing stress, which has to be applied to stretch the fibers in the drawing process.

#### Effect of Deformation Rate on "Apparent" Elongation Viscosity

Since the deformation rate has a marked influence on elongational viscosity,<sup>13,20</sup> a set of elongation experiments was performed at different tensile speeds and a constant drawing temperature. In Figure 7 the observed stress-strain curves are presented for the case of elongating fibers of material B at a drawing

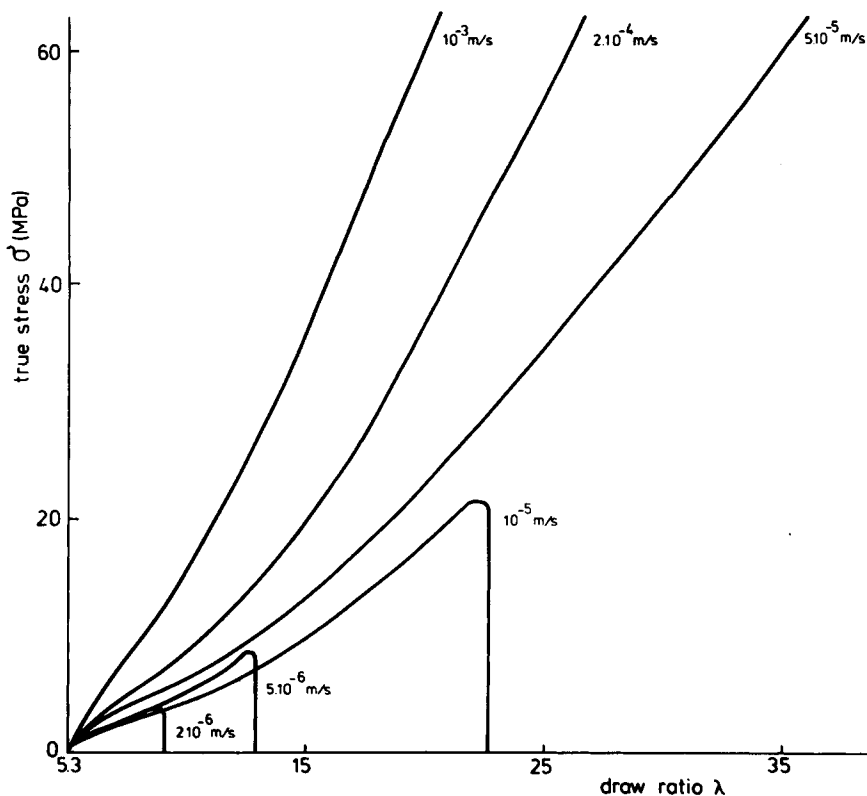


Fig. 7. Stress-strain curves for the elongation of porous polyethylene fibers (material B) at various tensile speeds and a drawing temperature of 124.5°C.

temperature of 124.5°C at various tensile speeds. It can be seen that the drawing behavior of the porous polyethylene fibers is strongly dependent on the rate of elongation. The rate of strain-hardening decreased with decreasing tensile speed. A striking feature of Figure 7 is the decrease of elongation at break with decreasing tensile speed. Similar behavior was noticed at higher temperatures. In Figure 8,  $\lambda_{\max}$  is plotted against tensile speed for material A at a temperature of 139.5°C and for fibers of material B at 124.5°C. It is frequently observed that during drawing of polymeric materials a decrease of tensile speed results in an increase of  $\lambda_{\max}$ . In fact, this common behavior was also observed for the usual hot drawing of the porous polyethylene fibers in the standard drawing apparatus, where drawing was performed at larger deformation rates than in the present study. As a result the anomalous behavior of  $\lambda_{\max}$  decreasing with decreasing tensile speed in the present study may originate from the fact that the available tensile speeds of the dynamometer resulted in very small deformation rates.

According to elongational flow theory,<sup>35,50</sup> drawing will only proceed effectively if the orienting action of the flow field prevails over relaxation phenomena, e.g., Brownian motion. This is expressed in the following condition

$$\dot{\epsilon} \cdot \tau_r > 1 \quad (15)$$

where  $\dot{\epsilon}$  is deformation rate and  $\tau_r$  is a characteristic relaxation time of the material. As the molecules become more extended, the tendency to recoil will grow

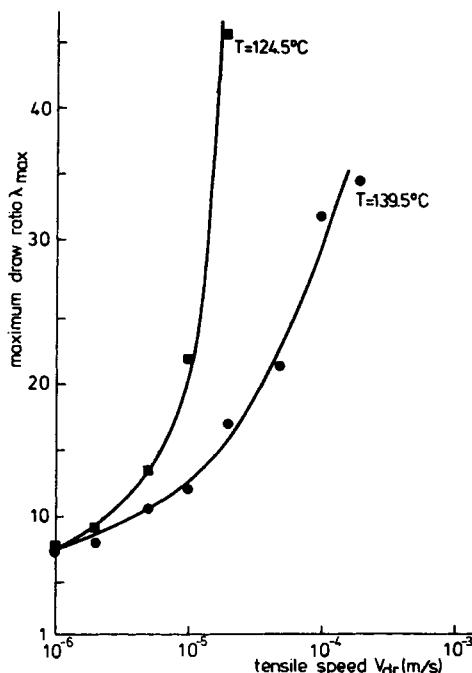


Fig. 8. Plot of maximum draw ratio  $\lambda_{max}$  vs. tensile speed  $V_{dr}$  for fiber material A at 139.5°C and material B at 124.5°C.

stronger, resulting in a shorter relaxation time. Furthermore, in the course of the drawing process the rate of deformation  $\dot{\epsilon}$  decreased with increasing draw ratio. Apparently the tensile speeds and thus the deformation rate during the dynamometer experiments were so small that, at a certain stage of the drawing process, relaxation phenomena started to dominate. As a consequence, partial melting of the fibers could occur, leading to failure of the samples. Hence, as the tensile speed was decreased, fiber breakage could occur at smaller values of  $\lambda$ . This is in accordance with the fact that  $\lambda_{max}$  for material B at 124.5°C increases considerably faster with increasing tensile speed than in the case of material A at 139.5°C due to the larger relaxation time in the former case.

“Apparent” elongational viscosity  $\eta_{\epsilon}$  vs. draw ratio  $\lambda$  during the hot drawing of fiber material A at 139.5°C for several tensile speeds is presented in Figure 9. At the highest stretching rates the “apparent” elongational viscosity strongly increases at small draw ratios followed by a leveling off at higher  $\lambda$ . For small tensile speeds in the range of  $10^{-6}$  m/s, however, the behavior of  $\eta_{\epsilon}$  with  $\lambda$  has strongly changed;  $\eta_{\epsilon}$  will even decrease at small  $\lambda$  followed by an upswing at higher draw ratio, illustrative of the extensive relaxation phenomena taking place in the fibers.

Finally  $\ln \eta_{\epsilon}$  was plotted against  $\ln \dot{\epsilon}$  in Figure 10 for some different values of  $\lambda$  for fiber material A at 139.5°C and material B at 124.5°C, showing a decrease of  $\ln \eta_{\epsilon}$  with increasing values of  $\ln \dot{\epsilon}$ . This observed behavior is commonly noticed for linear polyethylene melts.<sup>19,21,22</sup> Depending on the value of  $\lambda$ , a number of more or less parallel lines were noticed for both materials, though, in the case of material A,  $\ln \eta_{\epsilon}$  shows an upswing at low deformation rates.

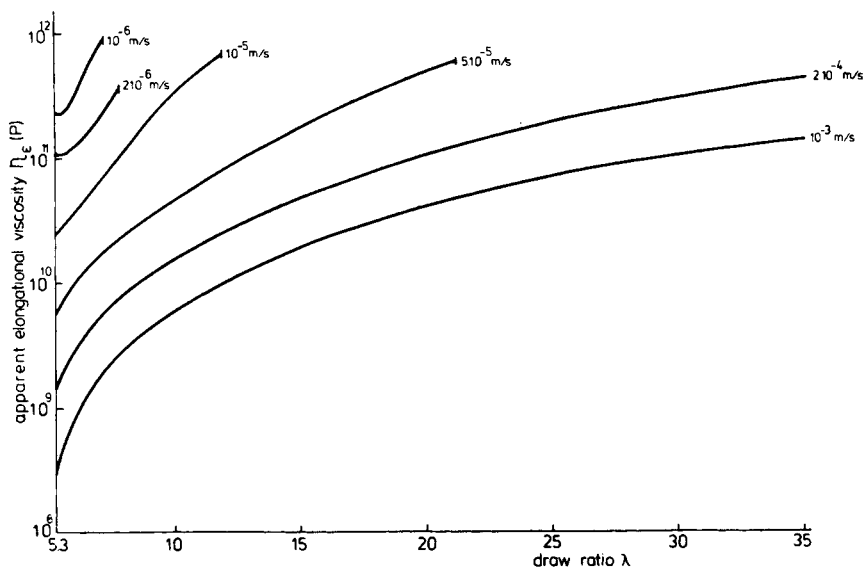


Fig. 9. "Apparent" elongational viscosity  $\eta_e$  vs. draw ratio  $\lambda$  at various tensile speeds upon drawing porous polyethylene fibers (material A) at  $T_{dr} = 139.5^\circ\text{C}$ .

DISCUSSION

The high tensile strength at break up to 4.1 GPa, which can be realized by hot drawing of porous high-molecular-weight polyethylene fibers, must originate from their molecular structure. It was recognized earlier<sup>51</sup> that orientation of high-molecular-weight polyethylene could lead to the formation of high strength structures, because of the reduced number of chain ends. Melt-processed high-molecular-weight polyethylene, however, shows only poor drawability,<sup>9</sup> even at elevated temperatures, due to the highly entangled, highly viscous network this material consists of. By starting from dilute solutions of the polyethylene, the amount of entanglements can be considerably reduced, and as a consequence the drawability of the fibers is greatly increased. Nevertheless,

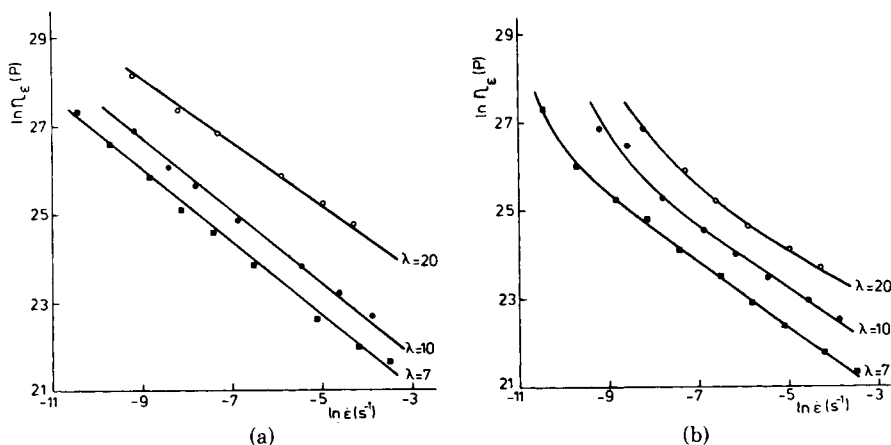


Fig. 10. Logarithm of "apparent" elongational viscosity in  $\eta_e$  vs. logarithm of deformation rate  $\ln \dot{\epsilon}$  upon drawing material B at  $124.5^\circ\text{C}$  (a) and material A at  $139.5^\circ\text{C}$  (b).

a minimum amount of entanglements is necessary in order to constitute a network that can be drawn out, and accordingly the minimum concentration of the polyethylene in solution is limited. A concentration high enough to give coil overlap is required. After spinning the solution at elevated temperature, the solution spun fibers are quenched to room temperature, upon which a large number of the entanglements become trapped by the crystallites. Subsequent extraction of the solvent leads to the formation of a loosely connected lamellar network with a high porosity.<sup>8</sup> In the hot-drawing process the original lamellar network is transformed into a highly oriented fibrillar structure. This general picture of the hot-drawing process has to be extended, since in this study it was observed that three different temperature regions for the activation processes involved in drawing have to be distinguished.

In the lowest temperature region up to 133°C the activation energy for the drawing process amounted to about 50 kJ/mol. The low  $E_a$  in this temperature range was clearly associated with the high porosity in the fiber, which was maintained throughout all stages of drawing. The high porosity probably results in a large free volume between the crystallites and accordingly lowers the energy barrier for transport of the molecules. In the early stages of drawing the folded chains of the lamellae start to be pulled out and a fibrillar structure is being formed. As a result of the low entanglement concentration, the unfolding of the lamellar crystals, which contain a large number of defects due to quench-crystallization, may proceed very effectively.<sup>52</sup> Presumably the transformation of the lamellae into fibrils occurred to a large extent during the predrawing of the fibers. The large increase of "apparent" elongational viscosity at small draw ratios up to  $\lambda = 8$  is probably also associated with this formation of the fibrillar structure together with the orientation of the fibrils parallel to the fiber axis. In subsequent stages of drawing in which  $\eta_e$  increases less pronouncedly with  $\lambda$ , the deformation probably proceeds by a sliding motion of separate fibrils past each other. As a consequence of the low activation energy, it seems highly improbable that individual chains are slipping past each other through the crystallites over long distances. Therefore, the main flow units in these stages of the hot drawing are presumably the separate fibrils. A further elongation of the molecules during drawing at higher values of  $\lambda$  may originate from the occurrence of weak spots in the originally formed fibrils. During the sliding motion of fibrils past each other, the fibrils can start to yield at these weak spots and thus a further extension of the molecules is accomplished by means of micronecking of the fibrils.

Above 133°C it was observed that the activation process involved in hot-drawing porous high-molecular-weight polyethylene definitely changes, resulting in a higher value for the activation energy of about 150 kJ/mol. Moreover, it was noticed that above this temperature the porosity of the fibers starts to decrease upon drawing. For small values of  $\lambda$  the distinction between the two regions above and below 133°C seemed to be less pronounced. In this drawing stage the fibrillar structure is being formed by pulling out of the folded chain lamellae, which apparently proceeds in more or less the same way in both regions. Heating experiments of "surface growth" polyethylene<sup>49</sup> fibers in SAXS revealed that fibrils start to aggregate above 135°C,<sup>53,54</sup> due to the fact that lamellar overgrowth situated alongside the fibrils is melted.

A similar event may take place during the drawing of the porous polyethylene fibers. Upon the formation of the fibrillar structure it may happen that the



major part of topological defects as entanglements, intertwinings, loose chain ends, etc. become situated on the outer part of the fibrils. Indications for this suggestion were obtained from transmission electron micrographs of transverse couples of hot-drawn porous high-molecular-weight fibers that were treated with chlorosulfonic acid and subsequently with uranylacetate.<sup>55</sup> It was observed that the cross section of each separate fibril, represented by light spots on the photograph, was surrounded by a more darkly colored ring of material that is preferentially attacked by the chlorosulfonic acid. This points again to the fact that on the outside of the fibrils a high defect concentration occurs. As the temperature rises above 133°C, partial melting can occur on the outside of the fibrils. During the sliding motion of fibrils the sticky, partially molten surfaces will increase the energy barrier for the drawing process.

In the temperature interval above 143°C the situation in the hot-drawing process has profoundly changed. A large activation energy was noticed, which was strongly dependent on the draw ratio. Moreover,  $E_a$  is affected by the initial morphology of the porous fibers in this region regarding the large differences found for material A and C. Above 143°C the mobility of the chains is sufficient to allow slippage of individual chains. The observed activation energies of 300–600 kJ/mol for material A and 180–250 kJ/mol for material C were in the same range as the activation energy calculated by Peterlin<sup>12</sup> for the integrated jumps of large chain parts. Therefore, it can be expected that hot drawing of the porous fibers above 143°C proceeds by slippage of individual molecules past each other with entanglements acting as semipermanent crosslinks between the molecules. On further increasing the draw ratio, more and more chains become fully stretched between entanglements, and, accordingly, the flow events become more integrated as  $\lambda$  increases, resulting in an increase of  $E_a$ . The more concentrated spinning solution for material A results in a larger entanglement concentration in this material as compared with material C, and, consequently, the activation energy will be larger for the former material.

The above-mentioned model for the drawing process suggests that the ultimate tensile strength of the fibers will be determined by the number of entanglements and other topological defects that occur in the structure, as they limit the extension of the molecules. Consequently, the ultimate tensile strength of fibers that are generated by the drawing technique may be intrinsically limited, as a minimum number of entanglements is necessary to stretch the molecules during drawing. In fact, in all experiments concerning the generation of ultrahigh-strength polyethylene fibers by means of hot drawing of porous high-molecular-weight polyethylene<sup>7,8</sup> as well as in the so-called "surface growth" technique,<sup>48,49</sup> an upper limit of the tensile strength was met at about 4.7 GPa. Polyethylene fibers with a tensile strength at break of about 3 GPa can be readily produced by these techniques, and, only if extreme care is taken, can tensile strength exceeding 4 GPa be realized. According to theoretical predictions,<sup>56</sup> the theoretical strength of polyethylene can reach a value of 66 GPa at 0 K, based on calculations concerning the strength of the C–C bond in polyethylene. Therefore, it seems that the ultimate strength of fibers produced by drawing techniques is intrinsically limited by the topological defect concentration.

Concerning the effect of deformation rate on the drawing properties of the porous polyethylene, it can be concluded that a strong reduction of the deformation rate to very small values (ca.  $10^{-6}$  m/s) probably affects the permanent

nature of the crosslinking action of the entanglements. The permanent character of the entanglements is presumably limited by the time scale of the hot drawing process. At very small tensile speeds, the diffusion of chain ends through entanglements may play an important role, according to a mechanism as suggested by Reneker.<sup>57</sup> As a result, loose chain ends are generated and extensive recoiling can occur. Hence partial melting of the fibers takes place, which leads to failure of the sample at a premature stage.

The behavior of  $\ln \eta_e$  vs.  $\ln \dot{\epsilon}$  during the hot drawing of the porous polyethylene fibers resulted in a number of more or less parallel lines, at various values of  $\lambda$ , revealing a decreasing "apparent" elongational viscosity with deformation rate. Surprisingly, the observed behavior shows a striking resemblance to the behavior of  $\ln \eta_e$  with  $\ln \dot{\epsilon}$ , as predicted by the model of Marrucci and Hermans<sup>32</sup> for polymer melts. This model was, however, strictly derived for the homogenous polymer melt and thus, strictly speaking, is not applicable to the hot-drawing behavior of the porous polyethylene, where the material exists in a nonhomogenous semicrystalline state. Nevertheless, there may exist some analogy between both cases if the flow behavior is looked at in terms of flow units, though the individual flow units must be quite different in both cases. In the Marrucci-Hermans<sup>32</sup> model a parameter  $B$  was introduced, a dimensionless quantity that defines the shape and mobility of the flow units. Different values of  $B$  result in parallel lines for the behavior of  $\ln \eta_e$  with  $\ln \dot{\epsilon}$ . Accordingly, an increasing value of  $\lambda$  during the hot drawing of the porous polyethylene might point to the fact, in correspondence with an increasing value of  $B$ , that the shape of the flow units becomes more elongated, which is in accordance with the micronecking behavior of fibrils and the extension of the molecules by the orienting action of the flow field.

Summarizing this discussion, we come to the conclusion that the hot drawing of porous high-molecular-weight polyethylene at temperatures below 143°C mainly proceeds by a sliding motion of elementary fibrils that were formed in the early stages of the drawing process. Above 133°C a change in activation energy was observed as it becomes possible for the elementary fibrils to aggregate. As temperature exceeds 143°C the mobility of the molecules is sufficient to allow slippage of individual chains in the course of the drawing process, with entanglements acting as semipermanent crosslinks. The ultimate strength of the hot-drawn polyethylene fibers is presumably limited by the topological defect concentration in the fibers. The permanent nature of the entanglements is limited by the time scale of the process.

Further observations on the morphology of the porous high-molecular-weight polyethylene fibers in the subsequent stages of the drawing process will be described in more detail in future publications.

This study was supported by the Netherlands Foundation for Chemical Research (SON) with financial aid from the Netherlands Organization for the Advancement of Pure Research (ZWO). The authors wish to express their gratitude to Dr. A. Eshuis for his assistance in the experimental and theoretical work. They also acknowledge valuable discussions with Prof. Dr. Ir. A. A. H. Drinkenburg and Prof. Dr. Ir. H. W. Hoogstraten, as well as with Dr. D. H. Reneker, N.B.S., and Dr. Joe le Blanc of the University of Massachusetts, Amherst.

## NOMENCLATURE

|                  |                                   |
|------------------|-----------------------------------|
| $\eta_0$         | zero shear viscosity              |
| $\eta_e$         | "apparent" elongational viscosity |
| $\dot{\epsilon}$ | deformation rate                  |
| $\lambda$        | draw ratio                        |
| $\tau$           | stress tensor                     |
| $\mathbf{D}$     | rate of deformation tensor        |
| $\sigma$         | axial tensile stress              |
| $F_{xx}$         | axial tensile force               |
| $A$              | cross section of the fibers       |
| $d$              | diameter of the fibers            |
| $E_a$            | activation energy                 |
| $T$              | drawing temperature               |
| $L$              | sample length                     |
| $v$              | tensile speed                     |
| $t$              | time                              |
| $\rho$           | density                           |
| $C_v, C_p$       | specific heat                     |
| $\Lambda$        | thermal conductivity              |
| $U$              | internal energy                   |
| $\alpha$         | heat transfer coefficient         |
| $\sigma_b$       | tensile strength at break         |
| $\tau_r$         | relaxation time of the material   |

## References

1. L. S. Singer, *Ultra-High Modulus Polymers*, A. Cifferri and I. M. Ward, Eds., Applied Science Publishers, London, 1979, p. 251.
2. J. R. Schaefgen, T. I. Bair, J. W. Ballou, S. L. Kwolek, P. W. Morgan, M. Panar, and J. Zimmerman, *Ultra-High Modulus Polymers*, A. Cifferri and I. M. Ward, Eds., Applied Science Publishers, London, 1979, p. 173.
3. M. G. Northolt, *Polymer*, **21**, 1199 (1980).
4. A. E. Zachariades, W. T. Mead, and R. S. Porter, *Ultra-High Modulus Polymers*, A. Cifferri and I. M. Ward, Eds., Applied Science Publishers, London, 1979, p. 77.
5. G. Capaccio and I. M. Ward, *Polymer*, **15**, 233 (1974).
6. B. Kalb and A. J. Pennings, *Polym. Bull.*, **1**, 871 (1979).
7. B. Kalb and A. J. Pennings, *J. Mater. Sci.*, **15**, 2584 (1980).
8. J. Smook, M. Flinterman, and A. J. Pennings, *Polym. Bull.*, **2**, 775 (1980).
9. G. Capaccio, T. A. Crompton, and I. M. Ward, *Polymer*, **17**, 644 (1980).
10. A. J. Pennings, *Macromol. Chem. Suppl.*, **2**, 99 (1979).
11. H. Eyring, *J. Chem. Phys.*, **4**, 283 (1936).
12. A. Peterlin, *Fracture*, **1**, 471 (1977).
13. C. D. Han, *Rheology in Polymer Processing*, Academic, New York, 1976.
14. M. Yamamoto, *J. Phys. Soc. Jpn.*, **12**, 1148 (1957).
15. A. S. Lodge, *Elastic Liquids*, Academic, New York, 1964.
16. J. L. White, *J. Appl. Polym. Sci.*, **8**, 1129 (1964).
17. M. C. Williams and R. B. Bird, *Phys. Fluids*, **5**, 1126 (1962).
18. T. W. Spriggs, *Chem. Eng. Sci.*, **20**, 931 (1965).
19. C. D. Han and R. R. Lamonte, *Trans. Soc. Rheol.*, **16**, 447 (1972).
20. F. T. Trouton, *Proc. R. Soc. London A*, **77**, 426 (1906).
21. J. L. White, *J. Appl. Polym. Sci.*, *Appl. Polym. Symp.*, **33**, 31 (1978).
22. Y. Ide, J. L. White, *J. Appl. Polym. Sci.*, **22**, 1061 (1978).
23. A. Ziabicki, *Kolloid-Z.Z. Polym.*, **175**, 14 (1961).
24. S. Kase and T. Matsuo, *J. Polym. Sci. A*, **3**, 2541 (1965).
25. D. Acierno, J. N. Dalton, J. M. Rodriguez, and J. L. White, *J. Appl. Polym. Sci.*, **15**, 2395 (1971).
26. R. R. Lamonte and C. D. Han, *J. Appl. Polym. Sci.*, **16**, 3285 (1972).
27. M. Doi and S. F. Edwards, *J. Chem. Soc. Faraday Trans., II*, **74**, 1789 (1978).

28. M. Doi and S. F. Edwards, *J. Chem. Soc. Faraday Trans., II*, **74**, 1802 (1978).
29. M. Doi and S. F. Edwards, *J. Chem. Soc. Faraday Trans., II*, **74**, 1818 (1978).
30. M. Doi and S. F. Edwards, *J. Chem. Soc. Faraday Trans., II*, **75**, 38 (1979).
31. P. G. de Gennes, *J. Chem. Phys.*, **55**, 572 (1971).
32. G. Marrucci and J. J. Hermans, *Macromolecules*, **13**, 380 (1980).
33. C. D. Han and L. Segal, *J. Appl. Polym. Sci.*, **14**, 2973 (1970).
34. A. Peterlin, *J. Mater. Sci.*, **6**, 490 (1971).
35. A. Ziabicki, *Fundamentals of Fibre Formation*, Wiley, London, New York, Sydney, Toronto, 1976, p. 402.
36. K. Koyama and O. Ishizuka, *Polym. J.*, **12**, 735 (1980).
37. W. T. Mead and R. S. Porter, *J. Polym. Sci., Polym. Symp.*, **63**, 289 (1978).
38. T. Kajiyama, T. Okada, A. Sakoda, and M. Takayanagi, *J. Macromol. Sci. Phys.*, **B7**, 583 (1973).
39. R. J. Cembrola and R. S. Stein, *J. Polym. Sci., Phys. Ed.*, **18**, 1065 (1980).
40. E. S. Clark and L. S. Scott, *Polym. Eng. Sci.*, **14**, 682 (1974).
41. D. H. Reneker, *J. Polym. Sci.*, **59**, S39 (1962).
42. A. Posthuma de Boer and A. J. Pennings, *Macromolecules*, **10**, 981 (1977).
43. I. Marshall, A. B. Thompson, *Proc. R. Soc. London A*, **221**, 541 (1954).
44. J. D. Ferry, *Viscoelastic Properties of Polymers*, Wiley, New York, London, 1970.
45. P. Zoller and H. Bont, *Polymer*, **15**, 239 (1974).
46. J. Brandrup and E. H. Immergut, *Polymer Handbook*, J. Brandrup and E. H. Immergut, Eds., Wiley, New York, London, Sydney, Toronto, 1975.
47. J. Smook, J. C. Torfs, P. F. van Hutten, and A. J. Pennings, *Polym. Bull.*, **2**, 293 (1980).
48. A. Zwijnenburg, Ph.D. thesis, State University of Groningen, Groningen, The Netherlands, 1978.
49. J. Smook, J. C. Torfs, and A. J. Pennings, *Makromol. Chem.*, **182**, 3351 (1981).
50. G. Marrucci, *Polym. Eng. Sci.*, **15**, 229 (1975).
51. P. J. Flory, *J. Am. Chem. Soc.*, **67**, 2048 (1945).
52. P. M. Tarin and E. L. Thomas, *Pol. Eng. Sci.*, **19**, 1017 (1979).
53. P. F. van Hutten, Ph.D. thesis, State University of Groningen, Groningen, The Netherlands, 1981.
54. P. F. van Hutten and A. J. Pennings, *Makromol. Chem. Rapid. Commun.*, **1**, 477 (1980).
55. J. Smook, B. A. Klazema, and A. J. Pennings, to appear.
56. D. H. Reneker and J. Mazur, *Polymer*, to appear.
57. B. Crist, M. A. Ratner, A. L. Brower, and J. R. Sabin, *J. Appl. Phys.*, **50**, 6048 (1979).

Received November 6, 1981

Accepted December 14, 1981